BENCHMARK
Journal of Cellular Biochemistry 115:1007–1022 (2014)

Journal of Cellular Biochemistry

Recent Advances in Thiol and Sulfide Reactive Probes

Ke Wang,[1] Hanjing Peng,[1,2] and Binghe Wang[1]*

[1]*Department of Chemistry and Center for Diagnostics and Therapeutics, Georgia State University, Atlanta 30303, Georgia, USA*

[2]*Department of Pharmacology and Molecular Sciences, Johns Hopkins University School of Medicine, Baltimore 21205, Maryland, USA*

ABSTRACT

Because of the biological relevance of thiols and sulfides such as cysteine, homocysteine, glutathione and hydrogen sulfide, their detection has attracted a great deal of research interest. Fluorescent probes are emerging as a new strategy for thiol and hydrogen sulfide analysis due to their high sensitivity, low cost, and ability to detect and image thiols in biological samples. In this short review, we have summarized recent advances in the development of thiol and hydrogen sulfide reactive fluorescent probes. These probes are compared and contrasted with regard to their designing strategies, mechanisms, photophysical properties, and/or reaction kinetics. Biological applications of these probes are also discussed. J. Cell. Biochem. 115: 1007–1022, 2014.

KEY WORDS: THIOL DETECTION; HYDROGEN SULFIDE; FLUORESCENT PROBES; CYSTEINE; HOMOCYSTEINE; GLUTATHIONE

Thiols, such as cysteine (Cys), homocysteine (Hcy) and glutathione (GSH) (Fig. 1), are indispensable functional molecules in the biological system due to the strong nucleophilicity and redox reactivity of the sulfhydryl group [Fava et al., 1956]. Thiols are ideal nucleophiles in enzyme functions, excellent sensors [Go and Jones, 2013] and mild buffering molecules for maintaining cellular redox states [Deneke, 2000; Murphy, 2012]. Fluctuations in thiol concentrations can indicate or even lead to a variety of cardiovascular disorders and neurodegenerative diseases. For example, circulating Hcy has been correlated with Alzheimer's disease [Clarke et al., 1998] and coronary artery diseases [Falk et al., 2001; Fung et al., 2001]. Excessive amount of total Hcy (tHcy) in the blood, hyperhomocysteinemia, is related to folate deficiency, which can lead to miscarriage [Makino et al., 2004] and various tumors [Ebbing et al., 2010]. Cys deficiency is associated with slow growth, and liver and skin damage [Chen et al., 2010]. High Cys concentration exhibits neurotoxicity [Janáky et al., 2000]. Decrease in GSH concentration was also shown to be associated to Parkinson's disease [Martin and Teismann, 2009]. As a result, accurate detection of these biological thiols is of great importance in both clinical and research practice.

By taking advantage of the unique chemical properties of the sulfhydryl group, such as strong nucleophilicity and low redox potential (−0.2~−0.3 V) [Sanadi et al., 1959; Jocelyn, 1967], general detection of thiols can be achieved using thiol reactive probes and electrochemical probes [Escobedo et al., 2006]. For determination of specific thiols, both detection methods can be coupled with different separation technology, such as chromatography and capillary electrophoresis (CE). Chemically derivatized thiols can also be selectively detected using mass spectrometry (MS). Due to the low redox potential of the sulfhydryl group, thiols (R-SH) are readily oxidized to their disulfide state. For example, more than 95% of total Hcy is in the oxidized form [Refsum et al., 2004], while only a very small amount is in the form of free thiol. Therefore, a reducing pre-treatment is usually required to convert all thiol species to their reduced forms before analysis of total thiol concentrations. Reducing agents such as dithiothreitol (DTT), tris(2-carboxyethyl) phosphine (TCEP) [Burns et al., 1991], or sodium borohydride ($NaBH_4$) can be used for the reduction of disulfide bonds. Because the chemical derivatization relies on the nucleophilicity of the sulfhydryl group (pK_a of SH in Cys [Mendel et al., 1965]: 8.15, Hcy: 8.7, GSH: 8.56), pH of the media is also an important factor affecting the reaction rates and outcomes. Basic buffer condition is often used to deprotonate sulfhydryl group and to accelerate the sensing reaction [Lai and Tseng, 2012; Wang et al., 2004]. For thiol reactive probes, numerous reaction types have been utilized, including nucleophilic substitution, Michael addition, cyclization, cleavage of disulfide bond, metal complexes coordination, and redox reactions.

Hydrogen sulfide (H_2S), a gaseous small molecule, is generated in the cell by enzymes such as cystathionine β-synthase (CBS) [Chen et al., 2004] and cystathionine γ-lyase (CSE) [Ishii et al., 2004]. Since hydrogen sulfide was recognized as one of the three important

*Correspondence to: Dr. Binghe Wang, Department of Chemistry and Center for Diagnostics and Therapeutics, Georgia State University, Atlanta 30302-4098, Georgia, USA. E-mail: wang@gsu.edu

Manuscript Received: 20 September 2013; Manuscript Accepted: 7 January 2014

Accepted manuscript online in Wiley Online Library (wileyonlinelibrary.com): 10 January 2014

DOI 10.1002/jcb.24762 • © 2014 Wiley Periodicals, Inc.

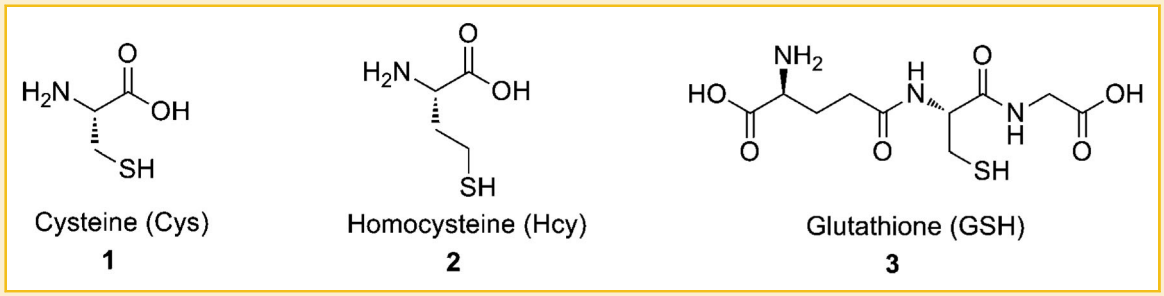

Fig. 1. Structures of Cysteine (Cys), Homocysteine (Hcy) and Glutathione (GSH).

TABLE I. Properties of Conventional Thiol Fluorescent Probes.

Entry	Probe	Compound number	Wavelength ($\lambda_{ex}/\lambda_{em}$, nm) or Abs.	Reaction time (min)	Temperature (°C)	pH	Medium	LOD	Application in biological system	Reference
1	mBB	**4**	380/ 480	2–20	25	7.4–8.9	N.D.	2 pM	Plasma	Chou et al., 2001; Nekrassova et al., 2003
2	Probe **7**	**7**	420/466	>60	N.D.	7.4	DMSO:HEPES 4:1	N.D.	Live cells	Kim et al. 2011
3	DNBSCy	**9**	600/700	30	N.D.	7.4	PBS	5 uM	Serum	Maity and Govindaraju, 2013
4	SSH-Mito	**13**	340/462& 545	120	37	N.D.	MOPS	N.D.	Live tissues, mitochondrial thiols	Lim et al., 2011
5	Ag-S-GF	N.D.	490/ 525	30	r.t.	N.D.	HEPES	6 nM	Buffer-diluted serum	Hu et al., 2011
6	NRFTP	**17**	470/ 510	30	r.t.	7.4	ACN/phosphate buffer 1:1.2	N.D.	Live cells	Long et al., 2011

N.D., not determined; mBB, monobromobimane; DMSO, dimethyl sulfoxide; HEPES, 4-(2-hydroxyethyl)-1-piperazineethanesulfonic acid; PBS, phosphate buffered saline; MOPS, 3-(*N*-morpholino) propanesulfonic acid.

gasotransmitters [Boehning and Snyder, 2003], there has been an interest in the improvement of its detection methods. Considering the features of hydrogen sulfide, such as reducing ability and duo-nucleophilicity (can undergo nucleophilic addition or substitution twice), current detection for hydrogen sulfide uses either sulfide specific chemosensor (methylene blue method) [Wei and Dasgupta, 1989], electrochemical methods (sulfide selective electrodes or polarographic methods) [Doeller et al., 2005; Schiavon et al., 1995] and gas chromatography (GC) [Ubuka et al., 2001]. However, none of these methods is compatible with detection and imaging in cells. These methods also show problems such as narrow linearity ranges (methylene blue method) and complicated sample preparations (chromatography). Recently, a number of fluorescent probes have been reported for the detection and imaging of H_2S [Lin and Chang, 2012; Peng et al., 2013; Peng et al., 2012]. This review mainly focuses on fluorescent probes developed in recent years for the detection of biological thiols and hydrogen sulfide.

CONVENTIONAL THIOL PROBES

Conventional non-selective thiol probes are used to detect, monitor or quantitatively evaluate all reactive SH groups in biological system with no or limited selectivity. Herein we provide a brief description of each type of fluorescent probes. Properties, such as excitation/emission wavelengths, reaction conditions, and limit of detection (LOD) of fluorescent conventional probes are summarized in Table I.

PROBES BASED ON NUCLEOPHILIC SUBSTITUTION

Based on the known nucleophilicity of the SH functional group, one of the classical and commercially available thiol detection reagents is monobromobimane (mBrB or mBB, compound **4**) (Fig. 2) [Chou et al., 2001; Ivanov et al., 2000a; Ivanov et al., 2000b]. It has been widely used in the determination of plasma tHcy in clinical applications [Chou et al., 2001]. Detailed description of mBB can be found in previous reviews [Nekrassova et al., 2003; Peng et al., 2012].

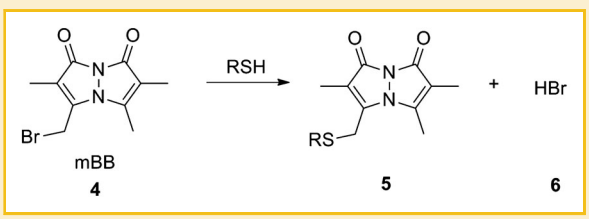

Fig. 2. Structure of probe mBB and its mechanism of action.

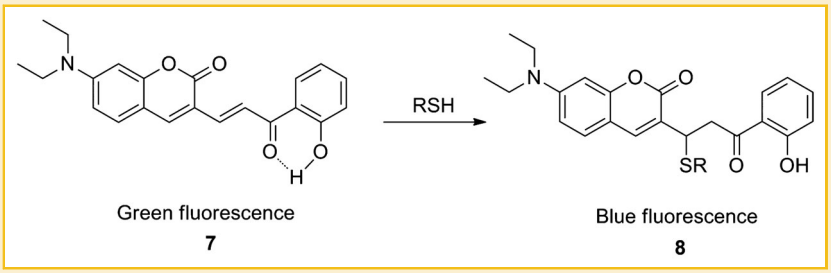

Fig. 3. Structure of probe **7** and its mechanism of action.

In 2011, a coumarin-based fluorescent probe (Compound **7**, Fig. 3) was reported by Kim and co-workers for cellular GSH imaging [Kim et al., 2011]. Through hydrogen bond-assisted Michael reaction, the probe ratiometrically responded to thiols by changing fluorescence from green to blue. Over 300-fold changes in fluorescence intensity ratio $I_{466\,nm}/I_{553\,nm}$ were observed with the addition of 10 mM (1000 equiv.) of biothiols in DMSO/HEPES (4-(2-hydroxyethyl)-1-piperazineethanesulfonic acid) (4:1). The detection limit was reported to be 37 μM for Hcy. Cellular GSH concentration can be measured using this ratiometric method. However, the requirement for large amount of DMSO as a co-solvent might be an issue for *in vivo* studies considering the cytotoxicity of DMSO.

Recently, near-infrared (NIR) probes have gained interest because of several unique advantages such as low excitation energy and deep tissue penetration [Frangioni, 2003]. A NIR fluorescent probe DNBSCy (**9**, Fig. 4) was reported by Covindaraju and co-workers. This probe is consisted of a sulfonyl ester thiol reactive moiety incorporated with a heptamethine cyanine (Cy) NIR dye, which can recover internal charge transfer (ICT) process after reacting with thiol and release thiol-dinitrobenzene (DNB) product. With the addition of thiols (1 mM), 10 μM of probe showed more than 20-fold fluorescence increase at 700 nm in phosphate buffered saline (PBS) and fetal bovine serum (FBS). The large Stokes shift (around 119 nm) of the NIR probe leads to high signal-to-noise (S/N) ratio and provides DNBSCy a low detection limit of 1 μM toward GSH in PBS buffer. As a result, this probe can be especially useful for monitoring the GSSG (GSH oxidized form)/GSH redox process in the presence of GSH reductase and NADPH (reduced form of nicotinamide adenine dinucleotide phosphate ($NADP^+$)) [Maity and Govindaraju, 2013].

PROBES BASED ON DISULFIDE BOND CLEAVAGE

Thiols exist in equilibrium between their reduced (thiol) and oxidized (disulfide) forms and can also react with other disulfides, forming new mixed disulfides and another free thiol. This property was used in the design of thiol reactive fluorescent probes. One of these examples was reported by Cho and co-workers. The fluorescent probe SSH-Mito (**13**) [Lim et al., 2011] was modified based on their first generation probe ASS (**14**) [Lee et al., 2010] (Fig. 5), which had stability problems, for mitochondrial thiol detection. Two-photon microscopy (TPM) was used in the detection. SSH-Mito is composed of 6-(benzo[*d*]thiazol-2′-yl)-2-(*N*,*N*-dimethylamino) naphthalene (BTDAN) as the reporter part, a disulfide bond as the thiol-reactive moiety [Long et al., 2011], and triphenylphosphonium salt (TPP) as the mitochondrial targeting site [Murphy and Smith, 2007]. In addition, to minimize the interaction between the disulfide bond and TPP, the structure was designed to separate them as far as possible. SSH-Mito shows a color change from blue to yellow in response to thiols with a change of the fluorescence intensity ratio (I_{yellow} to I_{blue}) by more than 42-fold in MOPS (3-(*N*-morpholino) propanesulfonic

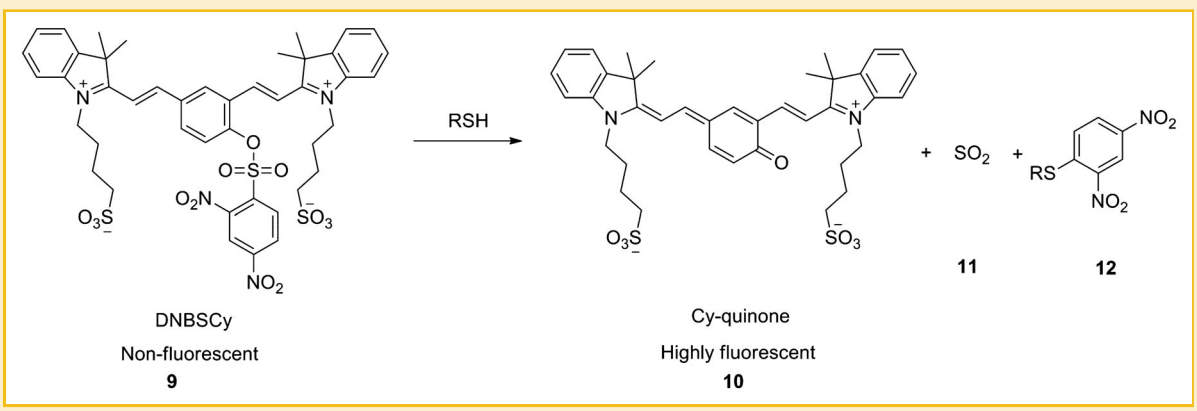

Fig. 4. Structure of probe DNBSCy and its mechanism of action.

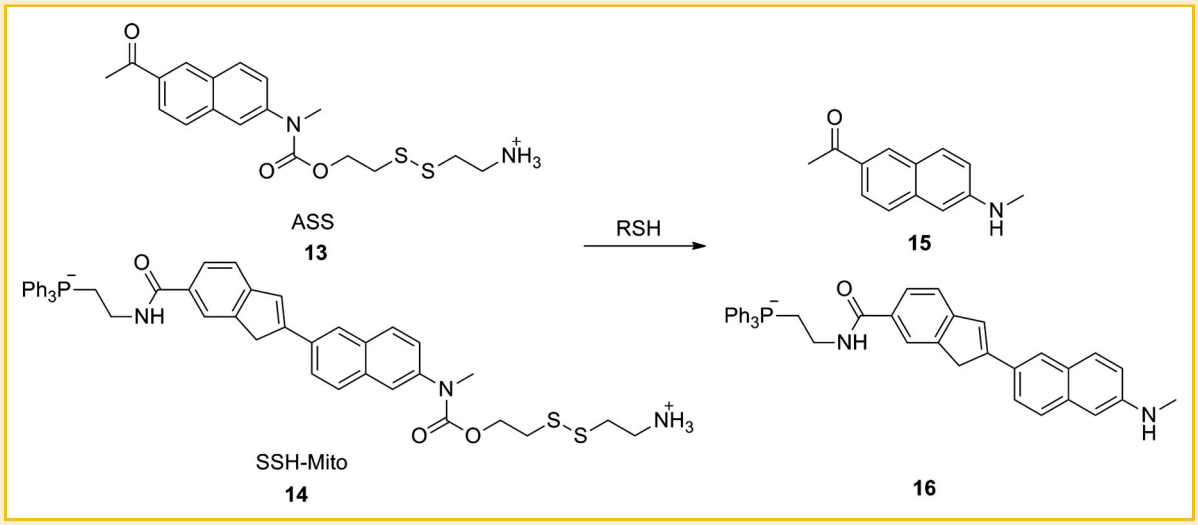

Fig. 5. Structure of probes ASS and SSH-Mito and their mechanisms of action.

acid) buffer. Further experiments using Cell Counting Kit-8 (CCK-8) indicate that SSH-Mito does not affect viability of cells. This probe can be applied in the ratiometric detection of mitochondrial thiols in live cells and tissues using TPM with penetration depth of more than 100 μM [Lim et al., 2011]. On the other hand, the solubility of SSH-Mito (5 μM in MOPS buffer) needs to be improved. Although it may be enough for cell staining, the solubility problem will limit its application.

PROBES BASED ON METAL–THIOL INTERACTIONS

Sulfur is known to have very strong intrinsic affinity for transition metals such as copper, mercury and silver, and thus is widely used as ligands in metal complexes [Vahrenkamp, 1975]. Therefore, transition metal-containing fluorescent probes were designed based on this property. A fluorescent turn-on method using Ag-S-GF (Fig. 6) was reported by Qu and co-workers in 2011. The design takes advantage of the metal binding properties of DNA [Becerril and Woolley, 2009] and the robust and specific interactions between sulfur and silver cation [Hu et al., 2011]. In this case, DNA was coated on silver surface via silver deposition. Then biological thiols and a DNA intercalating dye, GeneFinder (GF) [Pu et al., 2009], was added. Because Ag-S bond is much stronger than DNA-silver interaction, free DNA is released by thiol and binds with the intercalating dye, leading to a significant fluorescence increase [Lin et al., 2011]. Under optimized conditions (0.025 μM DNA, 3 μM $AgNO_3$ and 0.15 equiv., GeneFinder), the detection limit was around 6 nM, demonstrating excellent sensitivity. Experiments showed quantitative recovery in buffer-diluted fetal bovine serum. This assay is a simple, sensitive and selective detection method for biological thiols.

PROBES BASED ON NATIVE CHEMICAL LIGATION (NCL)

Native chemical ligation (NCL) is a commonly used reaction in peptide synthesis, with several advantages including compatibility with living cells [Dawson et al., 1994]. In 2011, a ratiometric on–off fluorescent probe based on Förster resonance energy transfer (FRET) was reported by Yuan and co-workers. The probe showed emission at

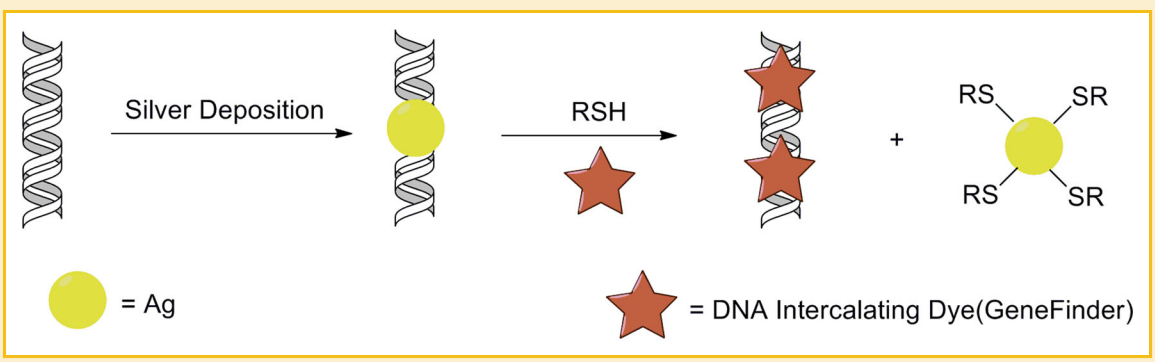

Fig. 6. Schematic presentation of probe Ag-S-GF assay and its mechanism of action.

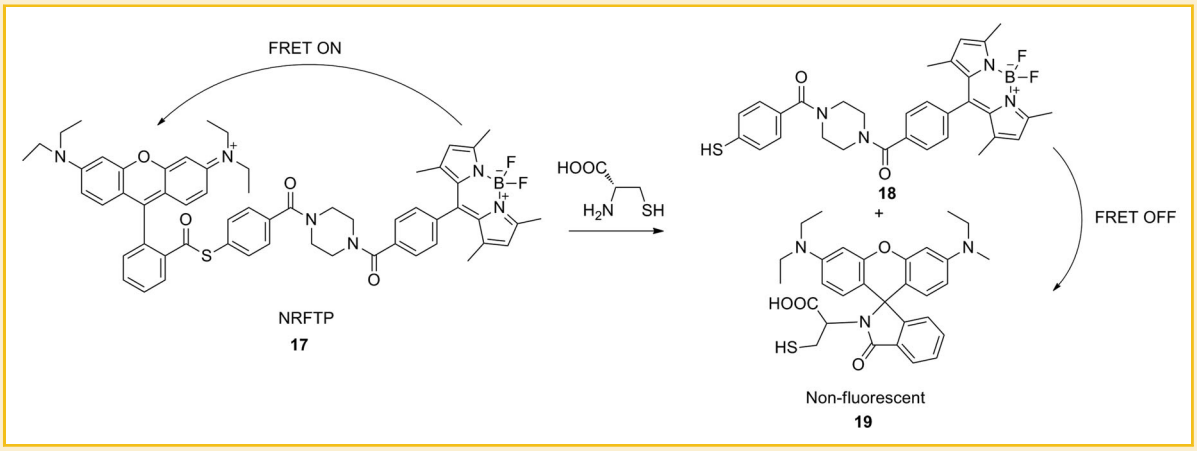

Fig. 7. Structure of probe NRFTP and its mechanism of action.

590 nm when excited at 470 nm (NRFTP, **17**, Fig. 7). When exposed to Cys, a native chemical ligation process dissociates the two fluorophores and turns the FRET off, leading to a blue shift in emission to 510 nm [Long et al., 2011]. In the presence of 100 μM Cys, the emission intensity at 510 nm increased by 275-fold. Within the linear correlation range from 0.1 μM to 100 μM, the detection limit of NRFTP was as low as 82 nM (S/N = 3) for Cys. In a methyl thiazolyl tetrazolium (MTT) cytotoxicity test, HeLa cells were incubated with this probe (2 μM) for 24 h. Less than 10% decrease of cell viability was observed, which was interpreted as having low toxicity. With this probe, one obvious drawback is the requirement for about 45% acetonitrile (ACN) as a co-solvent in phosphate buffer.

CYS/HCY-SPECIFIC PROBES

Cys and Hcy are two essential amino thiols (AT). Normal tHcy is lower than 15 μM in plasma, which is about 1/20 of the total Cys concentration [Refsum et al., 2004]. Considering the similarity and difference in structures, concentrations and biological functions between Cys and Hcy, tools capable of detecting and distinguishing these two thiols can be very useful. In this and the following sections, three classes of probes, Cys and Hcy-specific probes, Cys-specific probes, and Hcy-specific probes (Table II) are discussed.

Strongin and co-workers reported a thiazolidine reaction-based colormetric probe **20** (Fig. 8) in 2004, which can detect both Cys and Hcy with naked eyes. This probe has been reviewed in recently published reviews [Chen et al., 2010; Peng et al., 2012; Rusin et al., 2004; Wang et al., 2005]. As the very early Cys and Hcy probe, compound **20** shows a simple visual detection, but with drawbacks such as low sensitivity (LOD 1–10 μM) and insignificant absorbance changes (<15%) with thiol addition.

In 2010, Li reported an inorganic phosphorescent imaging probe, cationic iridium(III) complex (CIC, **22**) (Fig. 8), for Cys and Hcy detection in living cells. Upon addition of aminothiols, the probe's luminescence changes from yellow to red in DMSO–HEPES (9:1). This makes it a "naked-eye" indicator of Cys or Hcy. With its membrane-permeable property, CIC can ratiometrically indicate the intracellular Cys and Hcy concentrations. Furthermore, cytotoxicity of this probe was investigated using the MTT assay with human

TABLE II. Properties of Cys and Hcy Probes

Entry	Probe	Compound number	Specific detection analyte	Wavelength ($\lambda_{ex}/\lambda_{em}$, nm) or Abs.	Reaction time (min)	Temperature (°C)	pH	Medium	LOD	Application in biological system	Reference
7	Probe **20**	**20**	Cys/ Hcy	460/ 525	5	r.t.	9.5	H_2O	1–10 uM	Plasma	Rusin et al., 2004; Wang et al., 2005
8	CIC	**22**	Cys/ Hcy	430/547	30	37	7.2	DMSO: HEPES 9: 1	N.D.	N.D.	Xiong et al., 2010
9	Probe **24**	**24**	Cys	400 (Abs.)	10	r.t.	9.5	carbonate buffer	N.D.	N.D.	Wang et al., 2005
10	Probe **27**	**27**	Cys	304/ 377& 487	40	N.D.	7.4	EtOH/ phosphate buffer 2: 8	2–3 uM	Plasma	Yang et al., 2011
11	CyAC	**30**	Cys	365/ 520& 720	30	r.t.	7.4	EtOH/ HEPES 1: 9	N.D.	Live cells	Guo et al., 2012
12	Cd^{2+}-ACAQ	**32**	Cys	350/ 500	N.D.	25	7.4	HEPES	N.D.	N.D.	Zhou et al., 2011
13	MV^{2+}	**34**	Hcy	510 (Abs.)	5	r.t.	7.5	Tris	N.D.	Plasma	Wang et al., 2004
14	Fluorone black	**36**	Hcy	510 (Abs.)	5	r.t.	7.3	Phosphate buffer	N.D.	Plasma	Wang et al., 2004
15	FSN-AuNPs	N.D.	Hcy	370/ 485	120	r.t.	13	Phosphate buffer	4.4 nM	Plasma	Lai and Tseng, 2012

Tris, tris(hydroxymethyl) aminomethane.

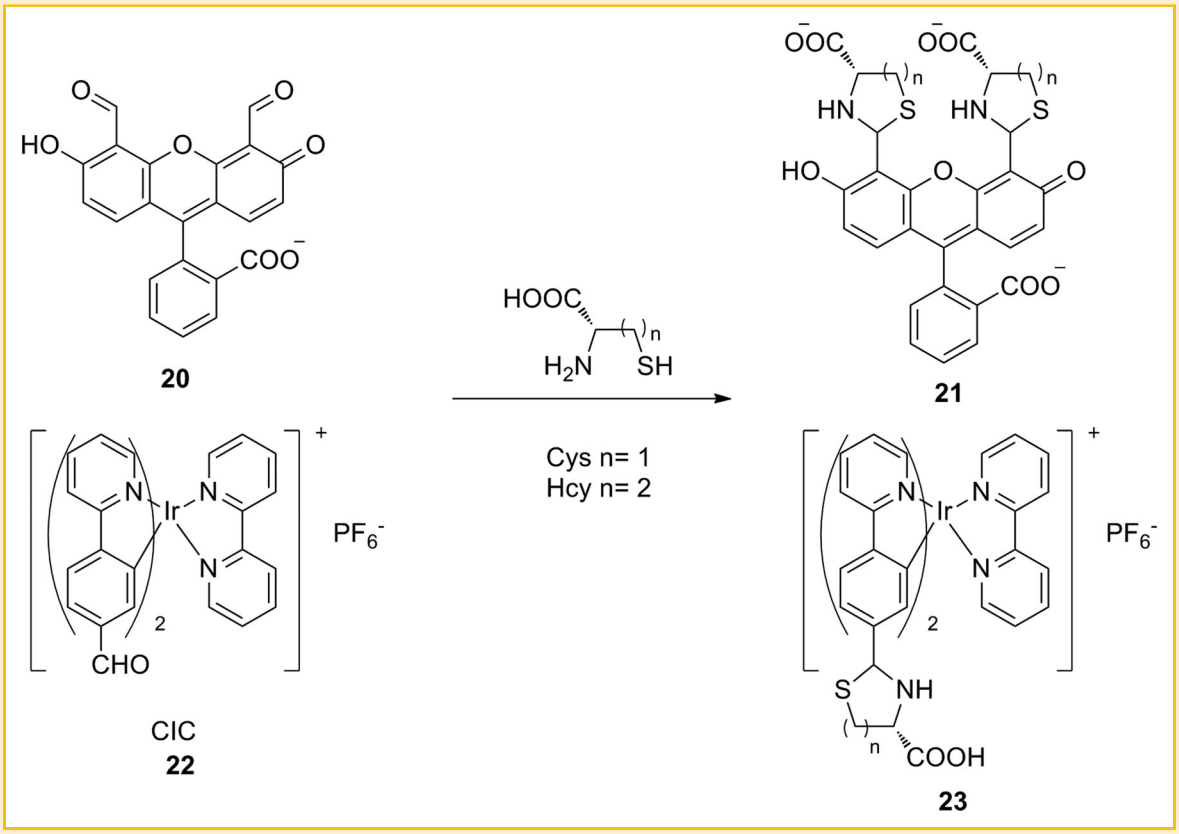

Fig. 8. Structures of Cys/Hcy-specific probes and their mechanisms.

nasopharyngeal epidermal carcinoma cell line (KB cells). In the presence of 100 μM probe CIC, the cellular viability was more than 80% after 24 h, indicating low cytotoxicity [Xiong et al., 2010].

CYS-SPECIFIC PROBES

PROBES BASED ON CONJUGATE CYCLIZATION

Based on the conjugate cyclization strategy, the Strongin group reported several Cys-specific fluorescent probes (Fig. 9) in 2005 and 2011 [Wang et al., 2005; Yang et al., 2011]. An α,β-unsaturated aldehyde, 4-(*N*,*N*-dimethylamino) cinnamaldehyde (compound **24**), and compound **27** showed Cys-specific detection based on kinetics difference in conjugate addition. These probes have been discussed in a recent review paper [Peng et al., 2012] and thus are not described in detail here.

A ratiometric NIR probe (CyAC, **30**) (Fig. 9) for Cys was reported by Yoon and co-workers in 2012. The mechanism for the selectivity between Cys and Hcy was also based on the kinetic difference in a cyclization reaction as described by Strongin and co-workers [Yang et al., 2011]. CyAC was designed based on a NIR hydroxy cyanine scaffold, which has intense absorption at 775 nm. With the addition of Cys, an obvious decrease (~20-fold) at 775 nm occurred, and a new peak at 515 nm with an isoemissive point at around 605 nm emerged. In the meanwhile, no response to the addition of Hcy and GSH was observed for this probe. With probe concentration at 5 μM, the pseudo-first-order rate constant for Cys (50 μM, 0.23 min^{-1}) was much higher than GSH (50 μM, 0.047 min^{-1}) and Hcy (50 μM, 0.029 min^{-1}). For biological applications, this probe can be used for fluorescence imaging of thiol in living cancer cells [Guo et al., 2012].

PROBES BASED ON Cys-METAL BINDING

D-Cys is known to be an inhibitor of *E. coli* growth [Soutourina et al., 2001]. In 2011, a fluorescent enantioselective chemosensor for D-Cys, a complex of cadmium and ACAQ (Cd^{2+}-ACAQ, **32**) (Fig. 10), was reported [Zhou et al., 2011a]. ACAQ was initially designed as a probe for Zn^{2+} and Cd^{2+}, with advantages of being cell permeable and capable of ratiometric detection [Zhou et al., 2011b]. Due to an ICT mechanism, metal-ACAQ complexation triggers a red-shift of the original emission band of ACAQ from 400 nm to 500 nm. With the addition of Cys, the cadmium complex (Cd^{2+}-ACAQ) shows a distinctive fluorescence decrease at 500 nm, a recovery ACAQ emission peak at 400 nm, and the formation of an isoemissive point at 450 nm in HEPES–ACN (2:8). It was suggested that the strong binding affinity of D-Cys and Cd^{2+} competes against metal-complex formation [Soutourina et al., 2001]; and thus in the presence of 5 equiv. of Cys, the emission spectrum is similar to that of ACAQ. The enantioselectivity was tested in different solvent systems. The best result $K_D/K_L = 3.35$ was obtained in 1% ACN/ HEPES. This probe also demonstrates selectivity to Cys over Hcy and GSH (~2-fold), although application with real biological samples was not described.

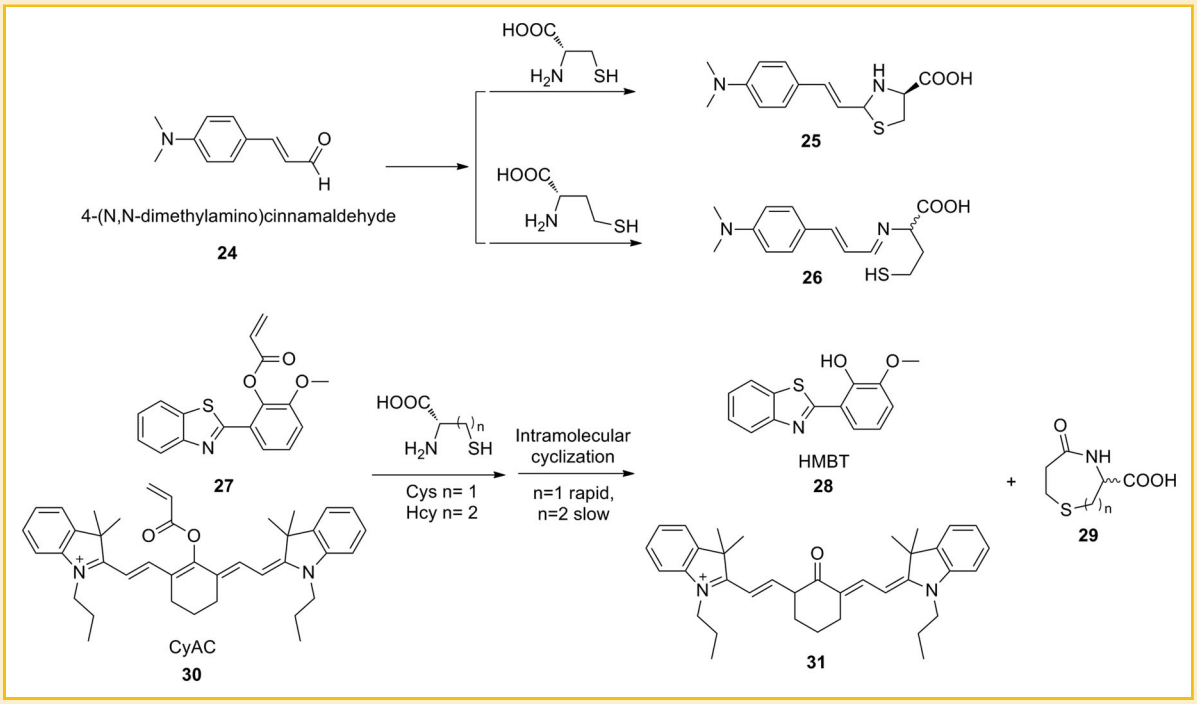

Fig. 9. Structures of cyclization-based probes and their mechanisms.

Hcy-SPECIFIC PROBES

Two Hcy-specific probes based on redox chemistry were reported by the Strongin group [Wang et al., 2004; Wang et al., 2005]. One visual detection probe was methyl viologen (MV^{2+}) (**34**, Fig. 11), which responded to Hcy changing from colorless to blue in 5 min. Another commercially available probe fluorone black (**36**, Fig. 11) shared a similar mechanism as that of MV^{2+} with higher detection sensitivity (linearity working range 0–15 μM). Both probes have been discussed in recent review [Peng et al., 2012] and thus are not in detail here.

Another quantitative detection method of Hcy in plasma was reported by Tseng and co-workers in 2012 [Lai and Tseng, 2012]. The combination of TCEP reduction, fluorosurfactant-capped gold nanoparticles (FSN-AuNP) extraction and subsequent *o*-phthaldialdehyde (OPA) derivatization (Fig. 12) provided a selective and sensitive method for quantification of total Hcy as well as protein-

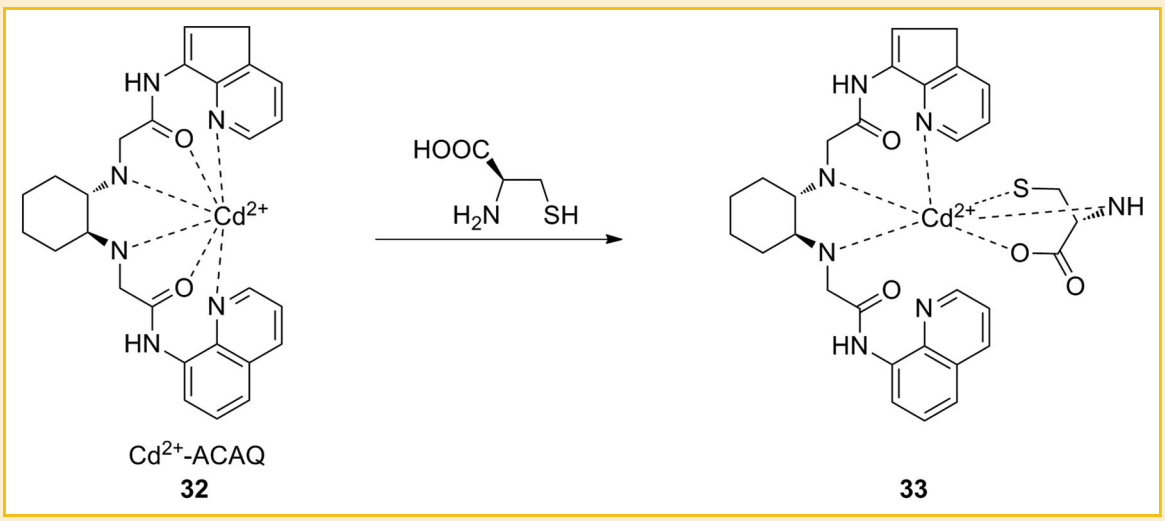

Fig. 10. Structure of probe Cd^{2+}-ACAQ and its mechanism of action.

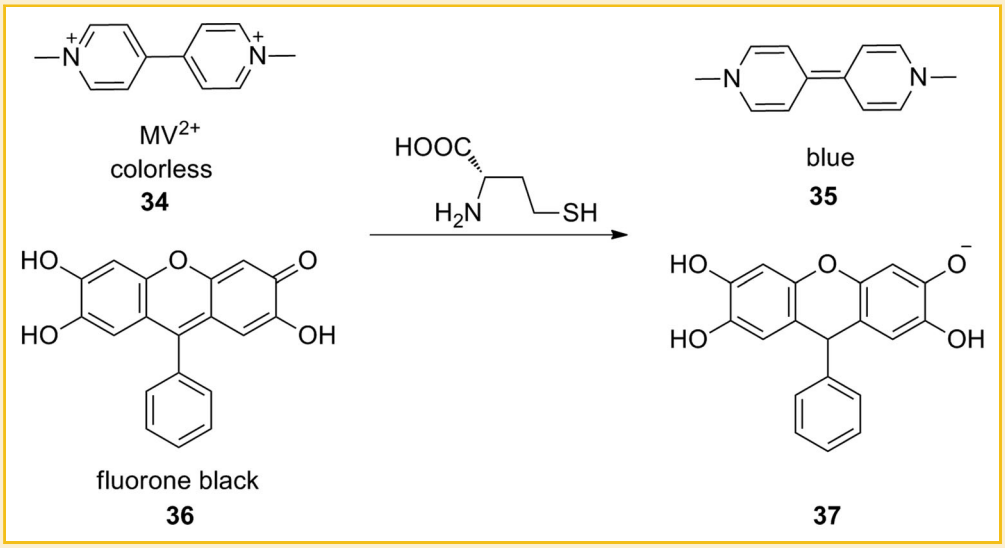

Fig. 11. Structures of Hcy-specific probes and their mechanisms of action.

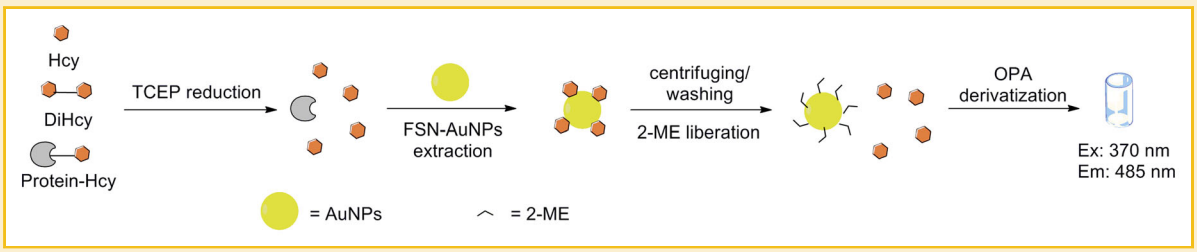

Fig. 12. Schematic presentation of probe FSN-AuNPs assay and its mechanism of action.

bound, free, and free oxidized Hcy. To avoid the interference of Cys, particle size of FSN-AuNPs was increased from 12 nm to 40 nm, which led to a higher aggregation rate of Hcy-attached AuNPs than Cys-attached [Lu and Zu, 2007]. In addition, OPA can selectively react with Hcy forming a highly fluorescent (9-fold intensity increase) product emitting at 485 nm with excitation at 370 nm [Chwatko and Jakubowski, 2005]. Within the dynamic range 0.01–1 μM, the detection limit of this method was determined to be 4.4 nM. This detection method can provide more than 100-fold selectivity toward Hcy over other aminothiols in plasma. However, the detection pH of this probe was 13, which cannot be widely used in detection in a biological system.

GSH PROBES

γ-L-Glutamyl-L-cysteinylglycine (GSH) is the most abundant non-protein aminothiols in cell [Hwang et al., 1992]. GSH and its disulfide oxidized form GSSG play an important role in redox homeostasis [Dalton et al., 1999]. To distinguish GSH from other aminothiols, selective probes have been developed (Table III).

TABLE III. Properties of GSH Probes

Entry	Probe	Compound number	Wavelength ($\lambda_{ex}/\lambda_{em}$, nm) or Abs.	Reaction time (min)	Temperature (°C)	pH	Medium	LOD	Application in biological system	Reference
16	mCB	**38**	380/470	30	r.t.	7.4	Tris	N.D.	Homogenates of rat livers	Kamencic et al., 2000
17	probe **39**	**39**	446/643	120	37	5.3–8.4	20% Ethanol–water	N.D.	Live cells	Shao et al., 2010
18	probe **41**	**41**	550/588	60	37	7.4	5% ACN–HEPES	86 nM	Live cells	Niu et al., 2012

mCB, monochlorobimane.

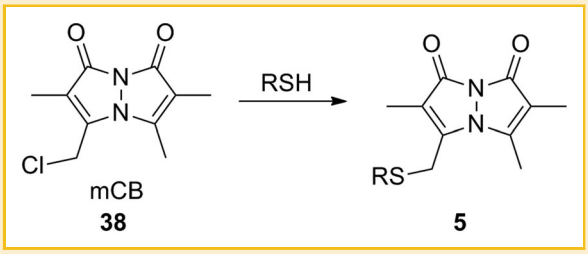

Fig. 13. Structure of probe mCB and its mechanism of action.

Monochlorobimane (mCB, **38**) (Fig. 13) [Fernández-Checa and Kaplowitz, 1990], which is an analogue of mBB, was reported as a GSH probe in early 1990s. Unlike mBB, it shows high (~5-fold) selectivity toward GSH. This probe was later used to determine the GSH content in rat liver [Kamencic et al., 2000].

In 2010, the Chan group reported a bis-spiropyran probe **39** (Fig. 14) with high selectivity toward GSH. This probe selectively binds with GSH with an affinity of 7.5×10^4 M^{-1}, leading to an increase in absorption at 446 nm (orange), which is 6-fold higher than that with Cys. In the presence of 1 mM GSH, this probe showed an 18-fold emission intensity increase at 643 nm. This probe is cell permeable due to its highly hydrophobic nature. As a result, it can be used for real-time monitoring of GSH in living cells with confocal fluorescence microscope [Shao et al., 2010].

A BODIPY-based GSH-selective probe **41** (Fig. 15) was reported by Yang and co-workers in 2012. The detection selectivity was achieved based on the different nucleophilicity of amino groups from aminothiol. Cys and Hcy can undergo two sequential reactions with monochlorinated BODIPY, while GSH can only react once, leading to different photophysical properties. This probe (10 μM) responded to 1 mM GSH by showing an 8-fold increase in emission at 588 nm, which discriminated GSH from Cys/Hcy. Within the GSH quantitative linear range (0–60 μM), the probe's detection limit was 86 nM. Cell imaging work indicated its cell permeability and GSH selectivity [Niu et al., 2012].

PROBES FOR HYDROGEN SULFIDE

H_2S has attracted great research interests and its detection is a hot topic in the sensing field in recent years. A few reviews have been published discussing H_2S probes [Lin and Chang, 2012; Pandey et al., 2012; Peng et al., 2013; Peng et al., 2012]. In this section, only recently published probes are included (Table IV).

PROBES BASED ON NUCLEOPHILIC REACTIONS

In aqueous solution, H_2S dissociates to form nucleophilic anion HS^-, which can react with a variety of electrophiles. Taking advantage of this feature, a number of probes have been developed. One of the examples is reported by Cui and co-workers with specific subcellular localization property [Liu et al., 2013b] (Fig. 16). This lysosome-targetable probe Lyso-NHS (**47**) consists of a 1,8-naphthalimide fluorophore, a 4-(2-aminoethyl) morpholine moiety (the lysosome targeting group), and a dinitrophenyl ether as the H_2S reactive site. In a mixed ACN/PBS (1:9) solvent, the probe was reported to react with excess amount (10 equiv.) of H_2S showing a 42-fold increase in emission at 555 nm. The limit of detection was 0.48 μM. Cytotoxicity was tested in MCF-7 cells. More than 90% cells survived after incubating with 5 μM of Lyso-NHS for 12 h.

Among all fluorescent probes, ratiometric probes afford easy quantification due to the advantage of self-calibration. In 2013, Z. Guo and co-workers reported a ratiometric H_2S probe CouMC (**49**, Fig. 17), for detection in mitochondria [Chen et al., 2013]. The selectivity for H_2S over Cys, Hcy and GSH is achieved due to differences in pK_a values. Biothiols have a higher pK_a (>8.5) [Lutolf et al., 2001] than H_2S (7.0), which makes H_2S a better nucleophile in neutral medium. Fluorescence titration of CouMC (10 μM) with NaHS (0–200 μM) resulted in a decrease in emission at 652 nm and an increase at 510 nm when excited at 475 nm. The intensity ratio I_{510}/I_{652} increased from 0.17 to 21.5, resulting in good sensitivity with LOD at around 1 μM. The reaction with NaHS at concentrations of 0–100 μM can be completed within 30 s, which is suitable for real-time detection of intracellular H_2S. Another ratiometric fluorescent probe flavylium derivative (compound **51**) was reported by W. Guo and co-workers recently (Fig. 17) [Liu et al., 2013a]. With a similar

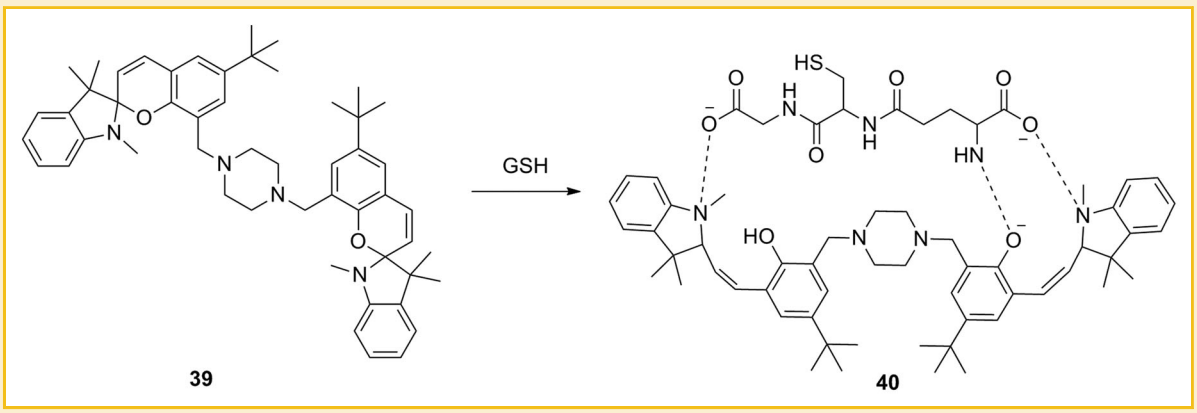

Fig. 14. Structure of probe **39** and its mechanism of action.

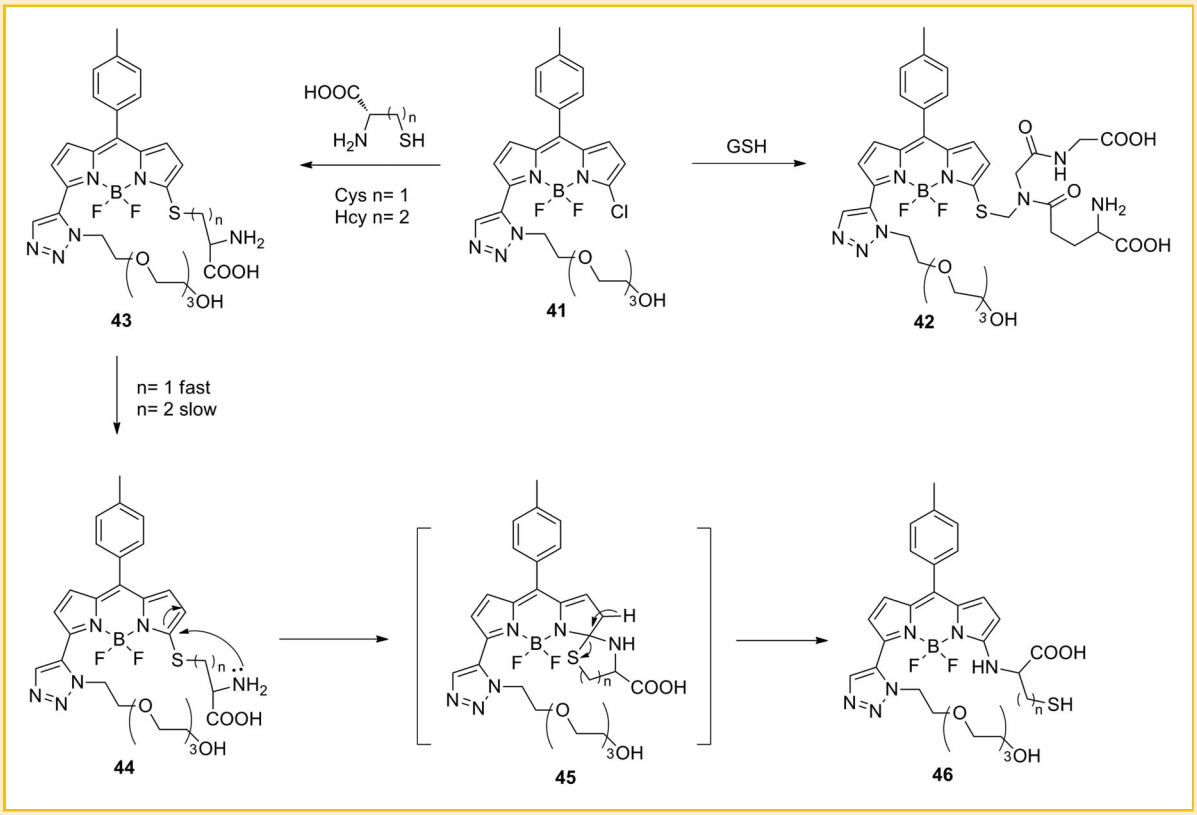

Fig. 15. Structure of probe **41** and its mechanism of action.

strategy, this probe featured a fast detection response (<10 s) and NIR property (λ_{em}: 485 and 690 nm) in ACN/PBS (1:3.3). MTT cytotoxicity studies using HeLa cells showed 80% cell viability after incubation with 10 μM probe for 24 h.

Further increased sensitivity was achieved by a NIR probe HS-Cy (compound **53**) reported by the Tang group (Fig. 17) [Wang et al., 2013d]. This probe takes advantage of the duo-nucleophilicity of hydrosulfide anion. It undergoes a nucleophilic addition by sulfide, followed by a thiolactone formation releasing a cyanine fluorophore. This resulted in an increase in emission at 780 nm and a decrease at 625 nm with the emission ratio (I_{625}/I_{780}) increasing from 0.01 to 24.8 with 14 equiv. of H_2S. The detection limit was as low as 5–10 nM. The application of this probe for detecting endogenous H_2S in human A549 cells was reported. However, the

TABLE IV. Properties of Hydrogen Sulfide Probes

Entry	Probe	Compound number	Wavelength ($\lambda_{ex}/\lambda_{em}$, nm) or Abs.	Reaction time (min)	Temperature (°C)	pH	Medium	LOD	Application in biological system	Reference
19	Lyso-NHS	**47**	450/555	20	37	7.4	ACN/PBS 1:9	0.48 uM	Serum and live cells	Liu et al., 2013b
20	CouMC	**49**	475/510 & 652	0.5	r.t.	7.4	2% DMSO–PBS	1 uM	Live cells	Chen et al., 2013
21	Probe **51**	**51**	450/485 & 690	0.17	r.t.	7.4	ACN/PBS 1: 3.3	0.14 uM	Live cells	Liu et al., 2013a
22	HS-Cy	**53**	510 & 700/625 & 780	35	37	7.4	HEPES	5–10 nM	Live cells	Wang et al., 2013d
23	Probe **57**	**57**	350/440, 510, & 570	30	37	7.4	DMSO: phosphate buffer 2:8	10 uM	Live cells	Wang et al., 2013c
24	SFP-1	**59**	300/395	60	37	7.4	PBS	5–10 uM	Live cells	Qian et al., 2011
25	SFP-2	**61**	465/510	240	37	7.0	PBS	6 uM	Live cells	Qian et al., 2011
26	SFP-3	**62**	500/525	30	25	7.4	PBS	1.5 uM	Plasma	Yong et al., 2012
27	SF4	**65**	496/517	60	25	7.4	HEPES	125 nM	Live cells	Lin et al., 2013
28	SF5-AM	**68**	498/521	60	25	7.4	HEPES	250 nM	Live cells	Lin et al., 2013
29	SF7-AM	**71**	498/526	60	25	7.4	HEPES	500 nM	Live cells	Lin et al., 2013
30	SHS-M1	**72**	365/500	90	r.t.	7.4	HEPES	200 nM	Live cells, tissue	Bae et al., 2013
31	SHS-M2	**73**	383/545	90	r.t.	7.4	HEPES	400 nM	Live cells, tissue	Bae et al., 2013
32	MPhSe-BOD	**75**	460/510	30	r.t.	7.4	PBS/ACN	<10 μM	Live cells	Wang et al., 2013c
33	Probe **77**	**77**	440/544	180	r.t.	7.4	Phosphate buffer	500 nM	Live cells	Xuan et al., 2012

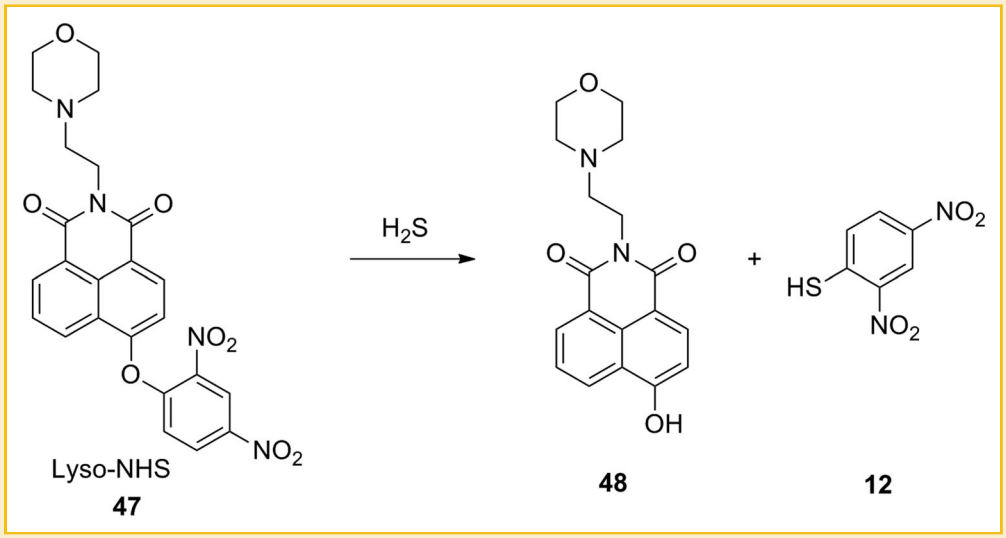

Fig. 16. Structure of probe Lyso-NHS and its mechanism of action.

reaction time (35-min reaction time) was long and not suitable for real-time detection.

A white light-emitting fluorescent probe (**57**) reported by Lin and co-workers shows advantages of low-background multi-channel detection (Fig. 18) [Wang et al., 2013c]. This probe was constructed by conjugating a blue fluorescent dye and with an ESIPT (excited-state intramolecular proton transfer) dye, which is modified by a 2,4-dinitrophenyl group as the reactive site. With the addition of NaHS, the probe responded with 3-, 6-, and 16-fold emission increases at 440 nm, 510 nm and 570 nm, respectively. The detection limit is 10 μM in phosphate/ DMSO 8:2 with 0.5% Tween-20. MTT assay in MG63 cells indicated more than 90% viability after incubated with 50 μM of the probe for 24 h. This probe can be utilized to detect endogenous H_2S in living cells with three-channel monitoring.

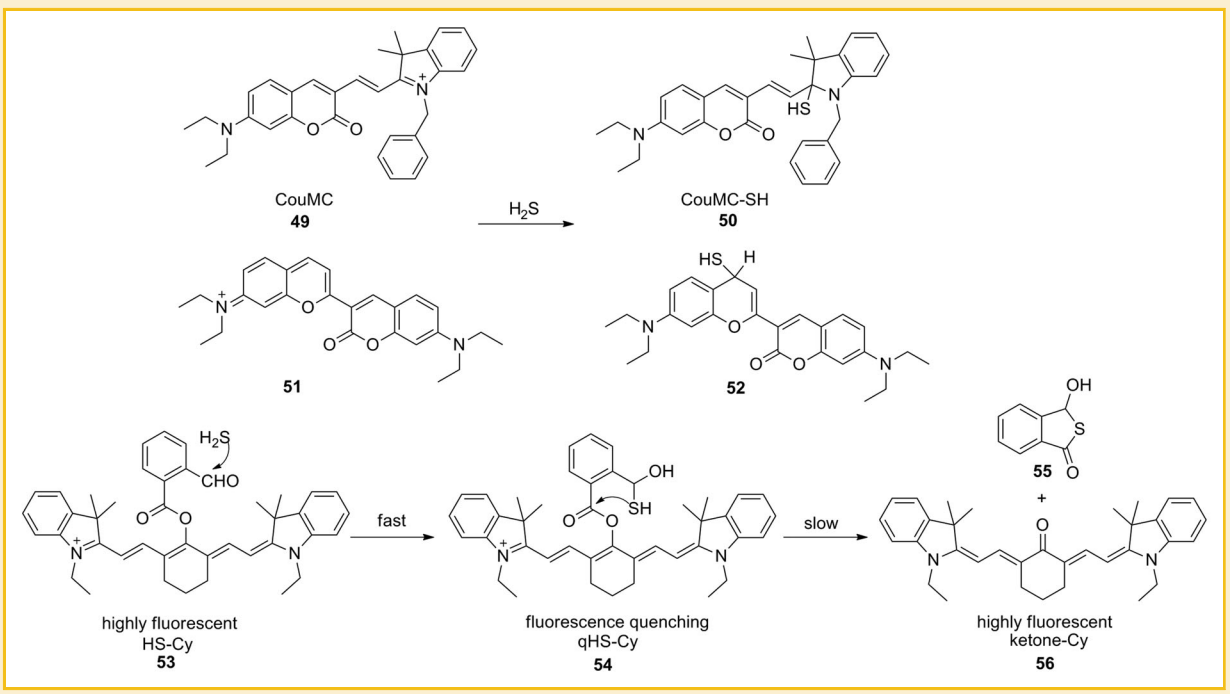

Fig. 17. Structure of ratiometric H_2S probes and their mechanisms of actions.

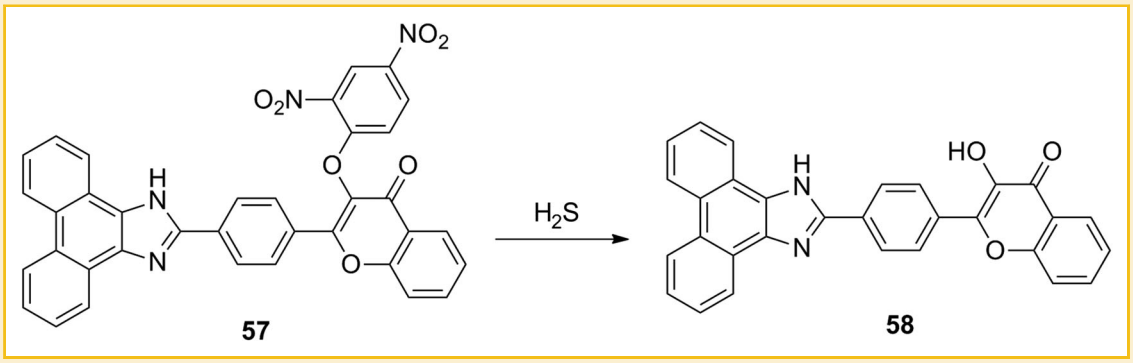

Fig. 18. Structure of probe 57 and its mechanism of action.

Although this probe is not as sensitive as some aforementioned probes, it features a new multi-channel sensor for hydrogen sulfide.

A series of hydrogen sulfide probes (SFP1, 2, 3, compounds **59, 61–62**, Fig. 19) were reported by the He group [Qian et al., 2011; Yong et al., 2012]. Based on a Michael addition–cyclization mechanism, these probes (5–10 μM) selectively react with sulfide exhibiting more than 10-fold fluorescence increases. Furthermore, SFP-1 and SFP-2 can be applied in dynamic monitoring of enzymatic hydrogen sulfide

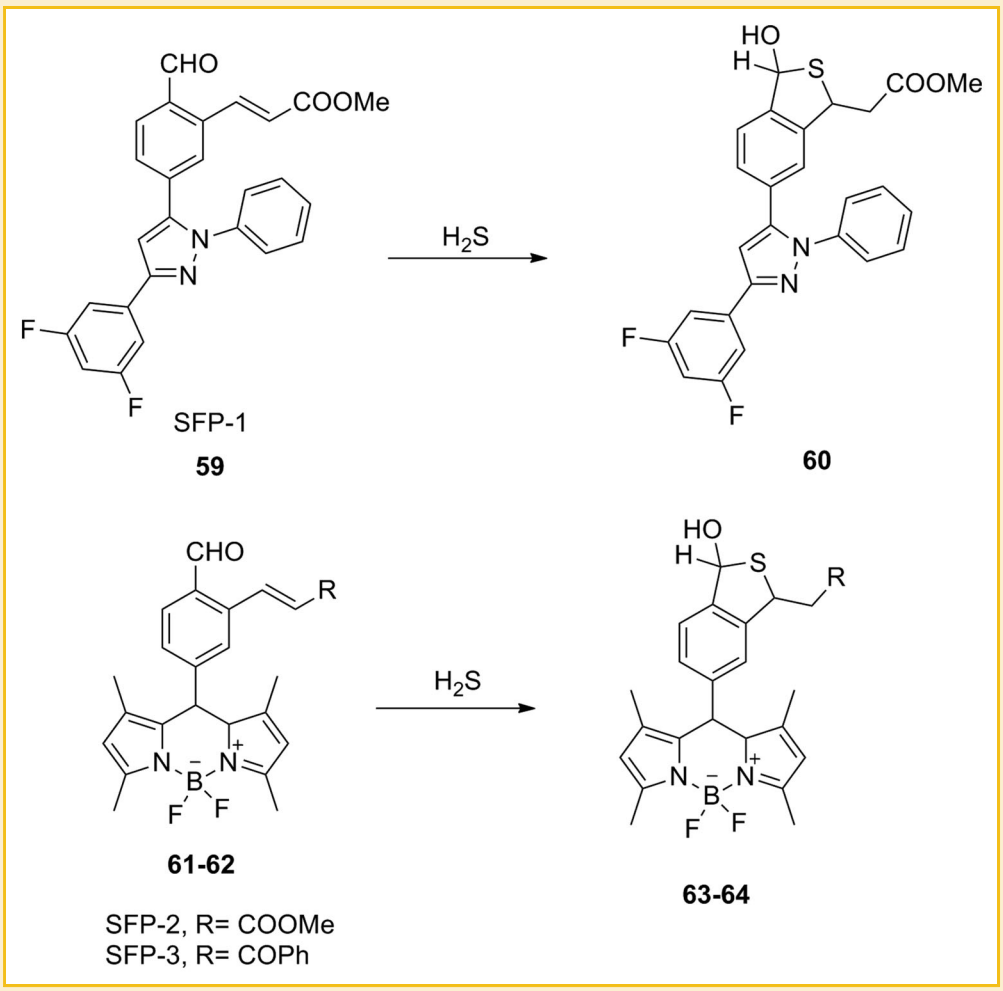

Fig. 19. Structures of SFP probes and its mechanism of action.

biosynthesis. These probes have been discussed in a previous review article [Peng et al., 2013] and thus not in detail here.

PROBES BASED ON REDOX REACTIONS

Hydrogen sulfide is a strong reducing agent. This feature has been utilized for developing a number of fluorescent probes. Chang [Lippert et al., 2011] and Wang [Peng et al., 2011] groups reported in 2011 the first fluorescent probes for H_2S based on the its ability to reduce the azido group and the rhodamine and dansyl fluorophores, respectively. Later more fluorescent probes have been reported based on this strategy. For fluorescent probes reported before 2012 the readers are referred to recent review articles [Lin and Chang, 2012; Peng et al., 2013; Peng et al., 2012].

In 2013, Chang and co-workers reported several bis-azido rhodamine analogues (SF4-SF7, compounds **65–69**, Fig. 20) for cell imaging of hydrogen sulfide [Lin et al., 2013]. Compared to the mono-azido probes reported in 2011, these bis-azido analogues exhibit improved sensitivity with detection limits ranging from 125–500 nM. Acetoxymethyl esters (SF5-AM, SF7-AM, compound **68**, **71**, etc.) were synthesized to provide cell-trappability for increased imaging sensitivity by maintaining a high dye concentration in the cells. Production of H_2S was observed in HUVECs (human umbilical vein endothelial cells) using SF7-AM and it was found that H_2S generation is dependent on NADPH oxidase (Nox) derived H_2O_2, providing evidence in support of H_2S/H_2O_2 crosstalk.

Ratiometric two-photon excitation fluorescent probes SHS-M1 and SHS-M2 (**72** and **73**, Fig. 20) were reported recently by Kim and co-workers [Bae et al., 2013]. The reduction of the 4-azidobenzyl group to the corresponding aniline triggers the cleavage of the carbamate, releasing the *N*-methylaniline analogues and resulting in a red shift from 420 to 500 nm for SHS-M1 and 464 to 545 nm for SHS-M2. This shift in emission provides feasibility for ratiometric detection of hydrogen sulfide for cellular imaging. The positively charged TPP serves as a mitochondria targeting moiety. SHS-M2 was used to monitor H_2S in cultured astrocytes and showed that H_2S production decreased when CBS was knocked down by siRNA. It was also found that H_2S level decreased in DJ-1-knockout astrocytes and brain slices as Parkinson's disease models.

A selenium-bearing fluorescent probe (MPhSe-BOD, **75**, Fig. 20) was reported by Han and co-workers [Wang et al., 2013b]. It exhibits a

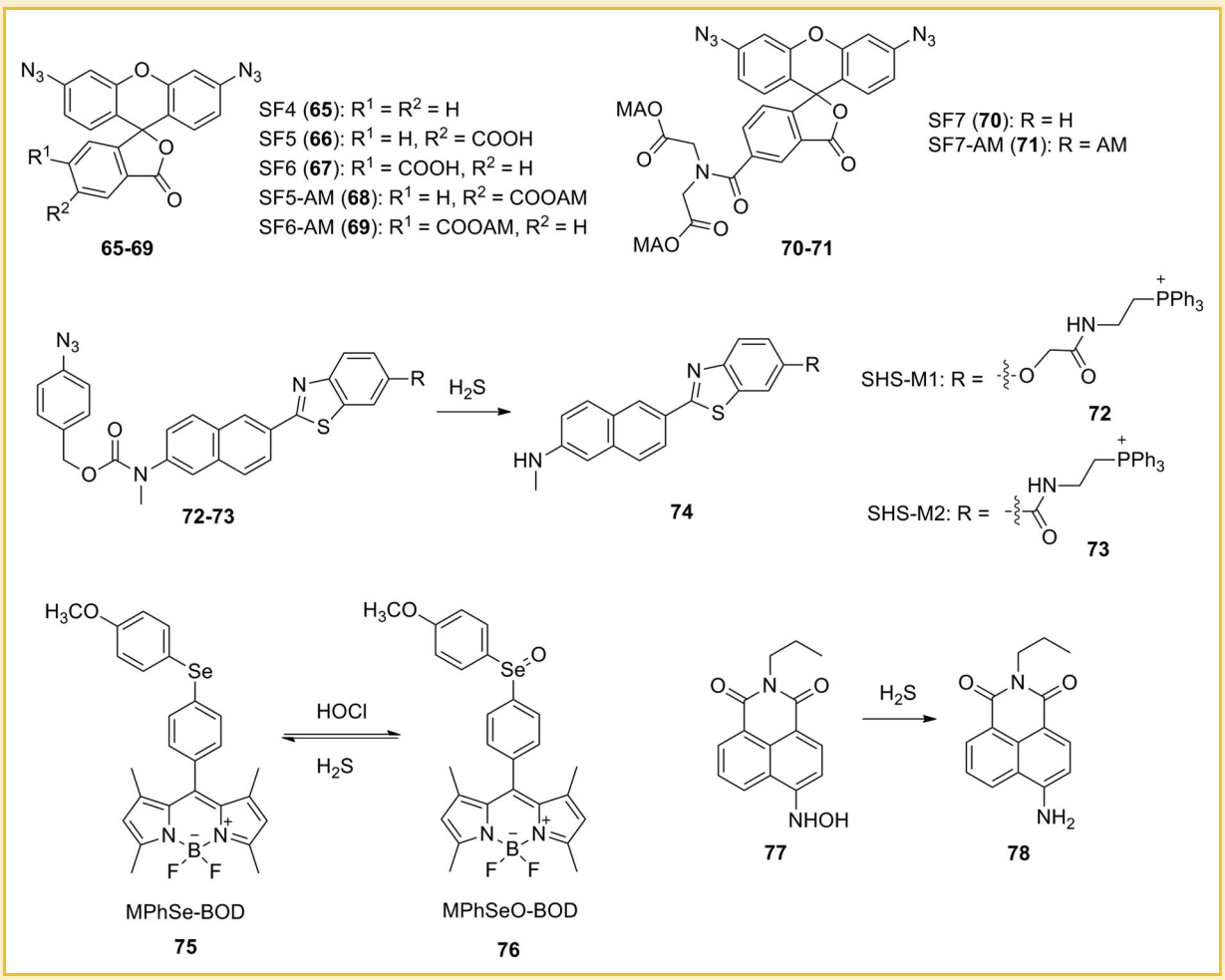

Fig. 20. Structure of redox-based H_2S probes and their mechanism of action.

reversible redox cycle between oxidation by hypochlorous acid (HClO) to MPhSeO-BOD (**76**, strongly fluorescent) and reduction by H_2S back to the original probe (weakly fluorescent). In a confocal imaging experiment, this probe showed good cell permeability in murine macrophage cell RAW264.7. It also showed the ability to continuously monitor the HClO/H_2S redox cycles when the production of hypochlorous acid (HClO) in cells was stimulated by phorbol myristate acetate (PMA) or exogenous sulfide was added into the cell culture. Similar strategy was also used in a NIR fluorescent probe reported by the same group [Wang et al., 2013a].

Another redox-sensitive naphthalimide-based fluorescent probe **77** (Fig. 20) was reported recently by Wang and co-workers [Xuan et al., 2012]. The reduction of hydroxylamine moiety by H_2S led to the production of its amino analogue as well as a dramatic increase in fluorescence intensity. A detection limit of sub-micromolar concentration was achieved. Imaging experiments in astrocytes using this probe revealed good cell membrane permeability. However, the slow kinetics (reaction requires 180 min to finish) hampers imaging applications.

A fluorescent protein (FP)-based hydrogen sulfide probe cpGFP-Tyr66pAzF was recently reported by the Ai group [Chen et al., 2012]. However, this was covered in a recent review [Peng et al., 2013] and thus is not discussed in detail here.

CONCLUSIONS

Thiols are important functional molecules in the biological system. Hydrogen sulfide has been recognized as a gasotransmitter and is involved in a number of cellular signaling pathways. New physiological and pathological implications of thiols and hydrogen sulfide have been revealed recently. Therefore, methods for accurate determination of thiols and H_2S are needed, especially for intracellular detection. A great deal of research efforts has been made to search for efficient and fast methods for thiol analysis. Fluorescent probes are emerging as new detection techniques due to their simple operation, low cost and most importantly, their compatibility with live cell imaging and possibility for real time monitoring. In this review, we have briefly introduced detection methods of thiols, with particular focus on thiol and sulfide reactive fluorescent probes developed in recent years. It is believed that these fluorescent probes will serve as powerful research tools in the study of thiols and hydrogen sulfide.

ACKNOWLEDGMENT

We are grateful for the financial support from Chinese Scholarship Council (KW), Molecular Basis of Disease Program for a fellowship (HP), and Center for Diagnostics and Therapeutics for a CDT/University fellowship (HP).

REFERENCE

Bae SK, Heo CH, Choi DJ, Sen D, Joe EH, Cho BR, Kim HM. 2013. A ratiometric two-photon fluorescent probe reveals reduction in mitochondrial H_2S production in parkinson's disease gene knockout astrocytes. J Am Chem Soc 135:9915–9923.

Becerril H, Woolley A. 2009. DNA-templated nanofabrication. Chem Soc Rev 38:329–337.

Boehning D, Snyder SH. 2003. Novel neural modulators. Annu Rev Neurosci 26:105–131.

Burns JA, Butler JC, Moran J, Whitesides GM. 1991. Selective reduction of disulfides by tris(2-carboxyethyl)phosphine. J Org Chem 56:2648–2650.

Chen S, Chen Z, Ren W, Ai H. 2012. Reaction-based genetically encoded fluorescent hydrogen sulfide sensors. J Am Chem Soc 134:9589–9592.

Chen X, Jhee KH, Kruger WD. 2004. Production of the neuromodulator H_2S by cystathionine beta-synthase via the condensation of cysteine and homocysteine. J Biol Chem 279:52082–52086.

Chen X, Zhou Y, Peng X, Yoon J. 2010. Fluorescent and colorimetric probes for detection of thiols. Chem Soc Rev 39:2120–2135.

Chen Y, Zhu C, Yang Z, Chen J, He Y, Jiao Y, He W, Qiu L, Cen J, Guo Z. 2013. A ratiometric fluorescent probe for rapid detection of hydrogen sulfide in mitochondria. Angew Chem Int Ed 52:1688–1691.

Chou S, Ko L, Yang C. 2001. High performance liquid chromatography with fluorimetric detection for the determination of total homocysteine in human plasma: method and clinical applications. Anal Chim Acta 429:331–336.

Chwatko G, Jakubowski H. 2005. The determination of homocysteine-thiolactone in human plasma. Anal Biochem 337:271–277.

Clarke R, Smith AD, Jobst KA, Refsum H, Sutton L, Ueland PM. 1998. Folate, vitamin B-12, and serum total homocysteine levels in confirmed Alzheimer disease. Arch Neurol 55:1449–1455.

Dalton T, Shertzer H, Puga A. 1999. Regulation of gene expression by reactive oxygen. Annu Rev Pharmacol Toxicol 39:67–101.

Dawson PE, Muir TW, Clarklewis I, Kent SBH. 1994. Synthesis of proteins by native chemical ligation. Science 266:776–779.

Deneke SM. 2000. Thiol-based antioxidants. Curr Top Cell Regul 36:151–180.

Doeller JE, Isbell TS, Benavides G, Koenitzer J, Patel H, Patel RP, Lancaster JR, Darley-Usmar VM, Kraus DW. 2005. Polarographic measurement of hydrogen sulfide production and consumption by mammalian tissues. Anal Biochem 341:40–51.

Ebbing M, Bùnaa K, Arnesen E, Ueland P, Nordrehaug J, Rasmussen K, Njùlstad I, Nilsen D, Refsum H, Tverdal A, Vollset S, Schirmer H, Bleie Ø, Steigen T, Midttun Ø, Fredriksen A, Pedersen E, Nygård O. 2010. Combined analyses and extended follow-up of two randomized controlled homocysteine-lowering B-vitamin trials. J Intern Med 268:367–382.

Escobedo J, Rusin O, Wang W, Alptürk O, Kim K, Xu X, Strongin R. 2006. Detection of Biological Thiols. In: Geddes C Lakowicz J editor., US: Springer. pp 139–162.

Falk E, Zhou J, Mùller J. 2001. Homocysteine and atherothrombosis. Lipids 36:3–11.

Fava A, Iliceto A, Camera E. 1956. Kinetics of the thiol/disulfide exchange. J Am Chem Soc 70:833–838.

Fernández-Checa J, Kaplowitz N. 1990. The use of monochlorobimane to determine hepatic GSH levels and synthesis. Anal Biochem 190:212–219.

Frangioni J. 2003. *In vivo* near-infrared fluorescence imaging. Curr Opin Chem Biol 7:626–634.

Fung T, Rimm E, Spiegelman D, Rifai N, Tofler G, Willett W, Hu F. 2001. Association between dietary patterns and plasma biomarkers of obesity and cardiovascular disease risk. Am J Clin Nutr 73:61–67.

Go YM, Jones DP. 2013. Thiol/disulfide redox states in signaling and sensing. Crit Rev Biochem Mol Biol 48:173–181.

Guo Z, Nam S, Park S, Yoon J. 2012. A highly selective ratiometric near-infrared fluorescent cyanine sensor for cysteine with remarkable shift and its application in bioimaging. Chem Sci 3:2760–2765.

Hu B, Zhao Y, Zhu H, Yu S. 2011. Selective chromogenic detection of thiol-containing biomolecules using carbonaceous nanospheres loaded with silver nanoparticles as carrier. ACS nano 5:3166–3171.

Hwang C, Sinskey AJ, Lodish HF. 1992. Oxidized redox state of glutathione in the endoplasmic-reticulum. Science 257:1496–1502.

Ishii I, Akahoshi N, Yu X, Kobayashi Y, Namekata K, Komaki G, Kimura H. 2004. Murine cystathionine gamma-lyase: complete cDNA and genomic sequences, promoter activity, tissue distribution and developmental expression. Biochem J 381:113–123.

Ivanov A, Nazimov I, Baratova L. 2000a. Determination of biologically active low-molecular-mass thiols in human blood. I. Fast qualitative and quantitative, gradient and isocratic reversed-phase high-performance liquid chromatography with photometric and fluorescence detection. J Chromatogr A 895:157–166.

Ivanov A, Nazimov I, Baratova L. 2000b. Qualitative and quantitative determination of biologically active low-molecular-mass thiols in human blood by reversed-phase high-performance liquid chromatography with photometry and fluorescence detection. J Chromatogr A 870:433–442.

Janáky R, Varga V, Hermann A, Saransaari P, Oja S. 2000. Mechanisms of L-cysteine neurotoxicity. Neurochem Res 25:1397–1405.

Jocelyn PC. 1967. The standard redox potential of cysteine–cystine from the thiol-disulphide exchange reaction with glutathione and lipoic acid. Eur J Biochem 2:327–331.

Kamencic H, Lyon A, Paterson P, Juurlink B. 2000. Monochlorobimane fluorometric method to measure tissue glutathione. Anal Biochem 286:35–37.

Kim GJ, Lee K, Kwon H, Kim HJ. 2011. Ratiometric fluorescence imaging of cellular glutathione. Org Lett 13:2799–2801.

Lai Y, Tseng W. 2012. Gold nanoparticle extraction followed by o-phthaldialdehyde derivatization for fluorescence sensing of different forms of homocysteine in plasma. Talanta 91:103–109.

Lee J, Lim C, Tian Y, Han J, Cho B. 2010. A two-photon fluorescent probe for thiols in live cells and tissues. J Am Chem Soc 132:1216–1217.

Lim C, Masanta G, Kim H, Han J, Kim H, Cho B. 2011. Ratiometric detection of mitochondrial thiols with a two-photon fluorescent probe. J Am Chem Soc 133:11132–11135.

Lin V, Chang C. 2012. Fluorescent probes for sensing and imaging biological hydrogen sulfide. Curr Opin Chem Biol 16:595–601.

Lin V, Lippert A, Chang C. 2013. Cell-trappable fluorescent probes for endogenous hydrogen sulfide signaling and imaging H_2O_2-dependent H_2S production. Proc Natl Acad Sci USA 110:7131–7135.

Lin Y, Tao Y, Ren J, Pu F, Qu X. 2011. Highly sensitive and selective detection of thiol-containing biomolecules using DNA-templated silver deposition. Biosens Bioelectron 28:339–343.

Lippert A, New E, Chang C. 2011. Reaction-based fluorescent probes for selective imaging of hydrogen sulfide in living cells. J Am Chem Soc 133:10078–10080.

Liu J, Sun Y-Q, Zhang J, Yang T, Cao J, Zhang L, Guo W. 2013a. A ratiometric fluorescent probe for biological signaling molecule H_2S: fast response and high selectivity. Chem Eur J 19:4717–4722.

Liu T, Xu Z, Spring D, Cui J. 2013b. A lysosome-targetable fluorescent probe for imaging hydrogen sulfide in living cells. Org Lett 15:2310–2313.

Long L, Lin W, Chen B, Gao W, Yuan L. 2011. Construction of a FRET-based ratiometric fluorescent thiol probe. Chem Commun 47:893–895.

Lu C, Zu Y. 2007. Specific detection of cysteine and homocysteine: recognizing one-methylene difference using fluorosurfactant-capped gold nanoparticles. Chem Commun 3871–3873.

Lutolf M, Tirelli N, Cerritelli S, Cavalli L, Hubbell J. 2001. Systematic modulation of Michael-type reactivity of thiols through the use of charged amino acids. Bioconjugate Chem 12:1051–1056.

Maity D, Govindaraju T. 2013. A turn-on NIR fluorescence and colourimetric cyanine probe for monitoring the thiol content in serum and the glutathione reductase assisted glutathione redox process. Org Biomol Chem 11:2098–2104.

Makino A, Nakanishi T, Sugiura-Ogasawara M, Ozaki Y, Suzumori N, Suzumori K. 2004. No association of C677T methylenetetrahydrofolate reductase and an endothelial nitric oxide synthase polymorphism with recurrent pregnancy loss. Am J Reprod Immunol 52:60–66.

Martin HL, Teismann P. 2009. Glutathione-a review on its role and significance in Parkinson's disease. Faseb J 23:3263–3272.

Mendel F, Cavins JF, Wall JS. 1965. Relative nucleophilic reactivities of amino groups and mercaptide ions in addition reactions with α,β-unsaturated compounds. J Am Chem Soc 87.

Murphy M. 2012. Mitochondrial thiols in antioxidant protection and redox signaling: distinct roles for glutathionylation and other thiol modifications. Antioxid Redox Signaling 16:476–495.

Murphy M, Smith R. 2007. Targeting antioxidants to mitochondria by conjugation to lipophilic cations. Annu Rev Pharmacol Toxicol 47:629–656.

Nekrassova O, Lawrence N, Compton R. 2003. Analytical determination of homocysteine: a review. Talanta 60:1085–1095.

Niu L, Guan Y, Chen Y, Wu L, Tung C, Yang Q. 2012. BODIPY-based ratiometric fluorescent sensor for highly selective detection of glutathione over cysteine and homocysteine. J Am Chem Soc 134:18928–18931.

Pandey SK, Kim KH, Tang KT. 2012. A review of sensor-based methods for monitoring hydrogen sulfide.. TrAC, Trends Anal Chem 32:87–99.

Peng H, Chen W, Burroughs S, Wang B. 2013. Recent advances in fluorescent probes for the detection of hydrogen sulfide. Curr Org Chem 17:641–653.

Peng H, Chen W, Cheng Y, Hakuna L, Strongin R, Wang B. 2012. Thiol reactive probes and chemosensors. Sensors (Basel) 12:15907–15946.

Peng H, Cheng Y, Dai C, King A, Predmore B, Lefer D, Wang B. 2011. A fluorescent probe for fast and quantitative detection of hydrogen sulfide in blood. Angew Chem Int Ed 50:9672–9675.

Pu F, Huang Z, Hu D, Ren J, Wang S, Qu X. 2009. Sensitive, selective and label-free protein detection using a smart polymeric transducer and aptamer/ligand system. Chem Commun 7357–7359.

Qian Y, Karpus J, Kabil O, Zhang S, Zhu H, Banerjee R, Zhao J, He C. 2011. Selective fluorescent probes for live-cell monitoring of sulphide. Nat commun 2:495.

Refsum H, Smith A, Ueland P, Nexo E, Clarke R, McPartlin J, Johnston C, Engbaek F, Schneede J, McPartlin C, Scott J. 2004. Facts and recommendations about total homocysteine determinations: an expert opinion. Clin Chem 50:3–32.

Rusin O, St Luce N, Agbaria R, Escobedo J, Jiang S, Warner I, Dawan F, Lian K, Strongin R. 2004. Visual detection of cysteine and homocysteine. J Am Chem Soc 126:438–439.

Sanadi DR, Langley M, Searls RL. 1959. α-Ketoglutaric dehydrogenase: VI. reversible oxidation of dihydrothioctamide by diphosphopyridine nucleotide. J Biol Chem 234:178–182.

Schiavon G, Zotti G, Toniolo R, Bontempelli G. 1995. Electrochemical detection of trace hydrogen-sulfide in gaseous samples by porous silver electrodes supported on ion-exchange membranes (solid polymer electrolytes). Anal Biochem 67:318–323.

Shao N, Jin J, Wang H, Zheng J, Yang R, Chan W, Abliz Z. 2010. Design of bis-spiropyran ligands as dipolar molecule receptors and application to *in vivo* glutathione fluorescent probes. J Am Chem Soc 132:725–736.

Soutourina J, Blanquet S, Plateau P. 2001. Role of D-cysteine desulfhydrase in the adaptation of Escherichia coli to D-cysteine. J Biol Chem 276:40864–40872.

Ubuka T, Abe T, Kajikawa R, Morino K. 2001. Determination of hydrogen sulfide and acid-labile sulfur in animal tissues by gas chromatography and ion chromatography. J Chromatogr B Biomed Sci Appl 757:31–37.

Vahrenkamp H. 1975. Sulfur atoms as ligands in metal complexes. Angew Chem Int Ed 14:322–329.

Wang B, Li P, Yu F, Chen J, Qu Z, Han K. 2013a. A near-infrared reversible and ratiometric fluorescent probe based on Se-BODIPY for the redox cycle mediated by hypobromous acid and hydrogen sulfide in living cells. Chem Commun 49:5790–5792.

Wang B, Li P, Yu F, Song P, Sun X, Yang S, Lou Z, Han K. 2013b. A reversible fluorescence probe based on Se-BODIPY for the redox cycle between HClO oxidative stress and H_2S repair in living cells. Chem Commun 49:1014–1016.

Wang J, Lin W, Li W. 2013c. Three-channel fluorescent sensing via organic white light-emitting dyes for detection of hydrogen sulfide in living cells. Biomaterials 34:7429–7436.

Wang W, Escobedo J, Lawrence C, Strongin R. 2004. Direct detection of homocysteine. J Am Chem Soc 126:3400–3401.

Wang W, Rusin O, Xu X, Kim K, Escobedo J, Fakayode S, Fletcher K, Lowry M, Schowalter C, Lawrence C, Fronczek F, Warner I, Strongin R. 2005. Detection of homocysteine and cysteine. J Am Chem Soc 127:15949–15958.

Wang X, Sun J, Zhang W, Ma X, Lv J, Tang B. 2013d. A near-infrared ratiometric fluorescent probe for rapid and highly sensitive imaging of endogenous hydrogen sulfide in living cells. Chem Sci 4:2551–2556.

Wei L, Dasgupta PK. 1989. Determination of sulfide and mercaptans in caustic scrubbing liquor. Anal Chim Acta 226:165–170.

Xiong L, Zhao Q, Chen H, Wu Y, Dong Z, Zhou Z, Li F. 2010. Phosphorescence imaging of homocysteine and cysteine in living cells based on a cationic iridium(III) complex. Inorg Chem 49:6402–6408.

Xuan W, Pan R, Cao Y, Liu K, Wang W. 2012. A fluorescent probe capable of detecting H2S at submicromolar concentrations in cells. Chem Commun 48:10669–10671.

Yang X, Guo Y, Strongin R. 2011. Conjugate addition/cyclization sequence enables selective and simultaneous fluorescence detection of cysteine and homocysteine. Angew Chem Int Ed 50:10690–10693.

Yong Q, Ling Z, Shuting D, Xin D, Chuan H, Xi Emily Z, HaiLiang Z, Jing Z. 2012. A fluorescent probe for rapid detection of hydrogen sulfide in blood plasma and brain tissues in mice. Chemical Science 3.

Zhou X, Chan W, Lee A, Yeung C. 2011a. Ratiometric fluorescent probe for enantioselective detection of D-cysteine in aqueous solution. Beilstein J Org Chem 7:1508–1515.

Zhou X, Lu Y, Zhu J, Chan W, Lee WM, Albert, Chan P, Wong NS, Ricky, Mak NK. 2011b. Ratiometric fluorescent Zn^{2+} chemosensor constructed by appending a pair of carboxamidoquinoline on 1,2-diaminocyclohexane scaffold. Tetrahedron 67:3412–3419.